Atmospheric Environment 45 (2011) 6526–6533

Contents lists available at SciVerse ScienceDirect

Atmospheric Environment

journal homepage: www.elsevier.com/locate/atmosenv

Aircraft emissions and local air quality impacts from takeoff activities at a large International Airport

Yifang Zhu, Elinor Fanning, Rong Chun Yu, Qunfang Zhang, John R. Froines*

Department of Environmental Health Sciences, University of California Los Angeles, 650 Charles E. Young Drive, Los Angeles, CA 90095, USA

ARTICLE INFO

Article history:
Received 21 April 2011
Received in revised form
17 August 2011
Accepted 19 August 2011

Keywords:
Ultrafine particles
Aircraft emissions
Los Angeles International Airport
Chemical speciation
Takeoff
Emission index

ABSTRACT

Real time number concentrations and size distributions of ultrafine particles (UFPs, diameter <100 nm) and time integrated black carbon, $PM_{2.5}$ mass, and chemical species were studied at the Los Angeles International Airport (LAX) and a background reference site. At LAX, data were collected at the blast fence (~140 m from the takeoff position) and five downwind sites up to 600 m from the takeoff runway and upwind of the 405 freeway. Size distributions of UFPs collected at the blast fence site showed very high number concentrations, with the highest numbers found at a particle size of approximately 14 nm. The highest spikes in the time series profile of UFP number concentrations were correlated with individual aircraft takeoff. Measurements indicate a more than 100-fold difference in particle number concentrations between the highest spikes during takeoffs and the lowest concentrations when no takeoff is occurring. Total UFP counts exceeded 10^7 particles cm^{-3} during some monitored takeoffs. Time averaged concentrations of $PM_{2.5}$ mass and two carbonyl compounds, formaldehyde and acrolein, were statistically elevated at the airport site relative to a background reference site. Peaks of 15 nm particles, associated with aircraft takeoffs, that occurred at the blast fence were matched with peaks observed 600 m downwind, with time lags of less than 1 min. The results of this study demonstrate that commercial aircraft at LAX emit large quantities of UFP at the lower end of currently measurable particle size ranges. The observed highly elevated UFP concentrations downwind of LAX associated with aircraft takeoff activities have significant exposure and possible health implications.

1. Introduction

Airborne particulate matter (PM) has been associated with a range of adverse health impacts including respiratory and cardiopulmonary effects, and lung cancer (Boldo et al., 2006; Li et al., 2003a; Pope and Dockery, 2006; Schwarze et al., 2006). Airports are important sources of PM in urban airsheds yet regulators and public health agencies have little data available that address the characteristics of PM emitted from aircraft and the potential impact of exposure and health in adjacent communities. Several studies have related direct emissions of PM, black carbon (BC), carbon monoxide (CO), nitrogen oxides (NO_x), and volatile organic compounds (VOCs) from aircraft to air quality problems and adverse health impacts in communities near airports (Garnier et al., 1997; Herndon et al., 2005; Yu et al., 2004). Ultrafine particles (UFP, diameter <100 nm), derived from combustion processes were not fully investigated in these studies. There is evidence that UFPs may pose greater health risks than larger particles per unit mass as the smaller UFPs contain high proportions of organic material particularly semi-volatile organic compounds, have larger surface area per unit mass and an ability to penetrate cells (Diapouli et al., 2007; Li et al., 2003b; Oberdorster et al., 2004).

In response to the increasing concern for exposure to airport-related pollutants, several recent studies were conducted to understand the emissions from airports and their potential impacts on local and regional air quality. Both physical and chemical characteristics of PM and gaseous pollutants have been reported for different commercial aircraft engine models in the recently Aircraft Particle Emissions Experiment (APEX) (Kinsey, 2009; Kinsey et al., 2010). Herndon and colleagues detected PM emissions from in-use commercial aircraft at two different airports and found the number, magnitude, and composition of the PM emissions were associated with the different operation conditions such as “ground idle” and “takeoff” (Herndon et al., 2005). Hasegawa and colleagues carried out an intensive aircraft- and ground-based measurements of 31 nm–5 μm particles to investigate vertical profiles of size-resolved PM in the urban atmosphere (Hasegawa et al., 2007). Recently, high airborne concentrations of UFPs were reported in

* Corresponding author. Tel.: +1 310 206 6141; fax: +1 310 206 9903.
E-mail address: jfroines@ucla.edu (J.R. Froines).

1352-2310/$ – see front matter © 2011 Elsevier Ltd. All rights reserved.
doi:10.1016/j.atmosenv.2011.08.062

communities downwind of Los Angeles International Airport (LAX) and Santa Monica Airport (SMA) in Southern California (Hu et al., 2009; Westerdahl et al., 2008). Distribution of particle numbers by size showed that maximum particle counts were in the 10–20 nm range, presumably deriving from fuel combustion. At airports, there are numerous sources of fuel combustion including aircraft takeoff and landing, idling, and diesel vehicles for material transfer and these sources will likely produce UFPs.

Although previous studies provide necessary data regarding airport-related PM emissions including UFPs, there is still a knowledge gap on the emission and transport of UFPs during the operation of individual aircraft. Characteristics and quantification of direct UFP emissions from aircraft activities and associated spatial impacts remain limited. There is even less knowledge of the chemical identification of the particle- and gas-phase pollutants from aircraft emissions. This study attempted to address this important data gap by characterizing UFP emissions and particle- and gas-phase chemical composition associated with LAX aircraft takeoff operations. These data will provide a basis for further in-depth studies including PM toxicology and health effect studies.

2. Methods

2.1. Description of the sampling sites

Los Angeles International Airport (LAX) is the world's fifth busiest passenger airport and ranks sixth in air cargo capacity. LAX is located at the western border of the South Coast Air Basin near the Pacific Ocean (N 33°56.55′, W 118°24.48′). Flights into and out of LAX typically proceed from east to west, with 96% of the departures to the west over the ocean and 94% of the arrivals landing from the east. Two runways are located to the north and two are to the south of the LAX central terminal complex. On average, 1700 to 2200 aircraft movements occur daily at LAX.

The sampling site was located at the east end of runway 25R at LAX (Fig. 1). Runway 25R is primarily used for aircraft taking off to the west, directly against the prevailing wind, and represents 40% of the total departures at LAX. Some aircraft arrive on runway 25R but departures dominate runway activity. The runway sampling location is ideally positioned to capture emissions from aircraft takeoff thrust. Planes initiate takeoff close to the sampling site and then accelerate westward down the runway and away from the sampling site. Three fences, called "blast fences", are positioned north to south across the end of runway 25R, and are designed to buffer the blast of jet exhaust associated with takeoff. Samples were also collected at five downwind locations, spaced at increasing distances from the blast fence up to 600 m and upwind from the 405 freeway to avoid freeway traffic confounding. During monitoring at each location, simultaneous monitoring was conducted at the blast fence for comparison. Fig. 1 illustrates the locations of the major and minor blast fences. The blast fence location is approximately 140 m from the point on the runway at which departing aircraft initiate takeoff.

An upwind sampling site in a residential area north of LAX was chosen as a reference location (Fig. 1). The site experiences a prevailing sea breeze, with no major PM sources upwind. There are two high schools nearby, which may introduce some bus emissions to the area. However, in generally, traffic is very light in this area. This monitoring site is operated by the South Coast Air Quality Management District (AQMD), who generously provided access for the duration of the study.

2.2. Sampling and instrumentation

Field sampling was performed during three time periods. The summer field study took place September 23–29, 2005. Sampling was performed over 24 h intervals continuously, starting at 12:00 pm on September 23 and ending at 14:00 pm on September 29, 2005. The winter field study, took place over five days from February 22 to March 2, 2006, was limited to the blast fence and upwind sites. The third phase of the field work, near field downwind study, focusing on spatial impact of takeoff emissions was conducted May 15–26, 2006. Only data collected under prevailing wind (eastward from the ocean) were used in the following data analysis to avoid potential contamination from traffic emissions on the 405 freeway.

Table 1 shows the sampling instruments and equipment used in this study. A Scanning Mobility Particle Sizer (SMPS, TSI Classifier model: 3080, DMA model; 3081/CPC 3025), measuring particles in sizes from 6.15 to 225 nm was used at the LAX blast fence. A second

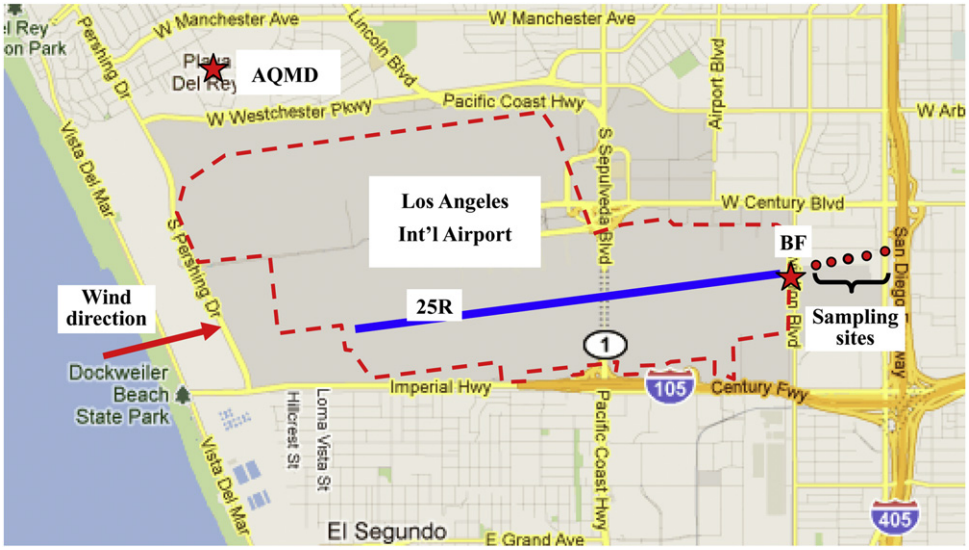

Fig. 1. Locations of background reference sites (AQMD) and study sites at LAX. Red marked sampling sites at blast fence (BF), 140 m distance from takeoff position, and additional five sampling locations 220 m, 250 m, 310 m, 410 m, and 610 m from the takeoff position. (For interpretation of the references to colour in this figure legend, the reader is referred to the web version of this article.)

Table 1
Instruments used in the study.

Pollutant (s)	Instrument (Supplier, Model)	Sampling Interval	Sampling Location (s)		
			Blast Fence	Further Downwind	Background Site
Particle Size Distribution	SMPS (DMA 3081)/CPC (3025) (TSI)	2 min	√		√
UFP Total or Size-specific Conc.	SMPS (DMA 3081)/CPC (3785) (TSI)	1 s	√	√	
Black Carbon	Aethalometers (Magee Scientific, AE-20)	5 or 10 min	√	√	
$PM_{2.5}$	E-BAM (Met One Instruments)	30 or 60 min	√		√
PAHs	Tisch Sampler (Tisch Environmental Inc. 1202)	~24 h	√		√
Butadiene/Benzene/Acrolein	Canister sampler	~24 h	√		√
Formaldehyde	Cartridge sampler	~24 h	√		√

Scanning Mobility Particle Sizer (SMPS, TSI Classifier model: 3080, DMA model: 3081/CPC 3785) was used to measure particle concentrations and size distributions, ranging from 7.64 to 289 nm at the AQMD background site. The two SMPSs were used to conduct near continuous monitoring by performing particle counts over short time intervals at the blast fence and further downwind sites simultaneously to better capture the spatial impacts of takeoff emissions. In these measurements, the DMA of the SMPS was adjusted to monitor a specific particle size and the CPC was used to count particle concentrations at the desired size every second, providing a real-time monitoring approach that could capture temporal variability in particle number concentrations. In the September study, monitoring was done for 7, 10, 20, 30, 50, 100, 150, and 200 nm on September 23 and at 8, 10, 15, 20, 30, 50, 75, 100, 150 and 200 nm particles on September 28. The monitoring time periods for 1 s scans lasted from 11 min to 77 min. During this period, CO_2 concentrations were also measured at the LAX blast fence by a Q-Trak IAQ monitor (Model 8550, TSI Inc., St. Paul., MN) at 1 min intervals, to facilitate emission index analysis (Section 3.3). In the winter study, similar 1 s scans were conducted for particles at 10, 15, 20, 30, 50, and 100 nm, on February 28, March 1 and 2. In the downwind study, 1 s data were simultaneously collected at 140, 220, 250, 310, 410 and 610 m downwind of the emission source.

Two Magee Scientific Aethalometers (Magee Scientific, model AE-20) were used to measure black carbon (BC) at the LAX blast fence and further downwind sites. The instruments were set up to measure average BC concentrations over 5 min intervals in the September study and over 10 min intervals in the winter study. E-BAMs (Met One Instruments) were used to measure $PM_{2.5}$ at the LAX blast fence and the background AQMD site during the September study. The instrument operated continuously for 168 h. During the same sampling period, Tisch Model 1202 samplers (Tisch, Cleves, OH) were deployed to obtain ambient samples of polycyclic aromatic hydrocarbon (PAH) species, and SUMMA polished stainless steel canisters were used to collect ambient air for chemical analysis for 1,3-butadiene, benzene, and acrolein at these two sites. Semi-volatile organic compounds including PAHs are known to be lost from filters during sampling and the undergo oxidation by ozone (Possanzini et al., 2006). The effect of these losses will be to underestimate airborne concentrations of organic compounds, but the magnitude could not be ascertained. The sampling train was the same as previously reported (Eiguren-Fernandez et al., 2004).

2.3. Data analysis

To analyze the highly resolved time vs. concentration data with respect to aircraft emissions, air traffic activity data were obtained from Los Angeles World Airports (LAWA). These data includes the logged departure time, arrival time, aircraft type, and airline identification number for flight activity at the runway. “Arrival” and “departure” time is logged by the control tower when a plane passes detection radar, and these logs times are not necessarily coincident with the time at which a plane and its emissions are closest to the sampling instruments. In order to investigate the specific impact of aircraft takeoffs on UFPs in each size range, the peaks in the particle concentration time profiles were matched with departure events from the airport logs, by manual inspection of the two related time series (concentration and aircraft activity). In addition, the data from selected takeoff events were used to model the aircraft emission during the complete cycle of an aircraft turning onto the runway, idling, and accelerating down the runway away from the blast fence sampling location, based on field notes collected during sampling.

The emission index of UFPs of a given measured sizes (EI_{pm}), defined as the particle number emission per unit mass of fuel burned, was calculated by:

$$EI_{\mathrm{pm}} = (\Delta x/\Delta \mathrm{CO_2}) \times EI(\mathrm{CO_2}) \times M_{\mathrm{air}}/M_{\mathrm{CO_2}} \times (1/\rho_{\mathrm{air}}) \quad (1)$$

WhereΔx is the incremental particle number concentration over background (particles cm^{-3}), ΔCO_2 is the incremental CO_2 concentration over background (ppm), $EI(CO_2)$ is 3160 g CO_2/(kg fuel), M_{air} and M_{CO_2} is the molar mass of air (29 g mol^{-1}) and CO_2 (44 g mol^{-1}) respectively, and ρ_{air} is the density of air (1.2 g L^{-1}) (Herndon et al., 2005). The SMPS data and CO_2 concentration collected on September 23, 2005 at blast fence were used to calculate EI_{pm} during aircraft takeoff events.

3. Results and discussion

3.1. UFP size distributions at the blast fence and background sites

SMPS data were averaged to yield an overall size distribution of particle number concentration at the blast fence site and the upwind background site (Fig. 2). In the September study, a total of

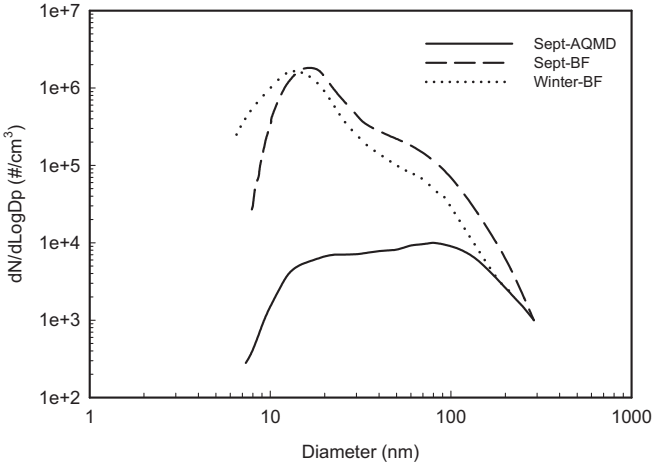

Fig. 2. Size distribution of UFP at near source (BF) and background (AQMD) sites, aggregated for each location/sampling time.

4639 SMPS scans were recorded at the blast fence and 5250 SMPS scans were recorded at the AQMD site. The size distribution for the winter campaign is based on 1100 2 min scans conducted on February 22, 23, and 24.

Fig. 2 shows that the distribution of particle size measured at the blast fence has the peak number concentration occurring in the nucleation range at 14 nm (dN/dlogDp = 1.4×10^6 particles cm^{-3}) in the summer study and 16.3 nm (dN/dlogDp = 1.3×10^6 particles cm^{-3}) during the winter study. A shoulder in the distributions between 50 and 90 nm indicates a slight secondary mode in the accumulation range, for both summer and winter studies. The concentration of particles smaller than the peak mode averages between 1.4×10^5 particles cm^{-3} to 1.4×10^6 particles cm^{-3} at the blast fence. Concentrations of particles larger than the mode decrease gradually with size, down to about 2×10^3 particles cm^{-3} for 255 nm particles. Slight differences in the size distributions between September and the winter sampling campaigns may be the result of different meteorology conditions.

At the AQMD background site, the size distribution is substantially different. Particle number concentrations are lower throughout the size range and the distribution of particles by size is notably different from that at the blast fence. The defined peak in the 14–16 nm size range that characterizes the near source location is absent from the background reference site. At the background site, particles are more evenly distributed across the size range, with a weakly defined peak mode at about 80 nm.

Data shown in Fig. 2 indicate that commercial aircraft takeoff activities at LAX emit large quantities of UFPs, especially in the nanometer (<50 nm) size range. These results are in excellent agreement with previous studies conducted near the LAX (Westerdahl et al., 2005) as well as at other airports (Herndon et al., 2005; Hu et al., 2009).

3.2. Temporal profile of UFPs at the blast fence site

To further investigate the contribution of takeoff activities to UFP emissions, size specific particle counts over 1 s intervals were measured by setting the DMA of the SMPS to a fixed particle size, to capture changes in particle concentration due to isolated aircraft takeoff events. A typical example of a takeoff cycle is shown in Fig. 3, which depicts the time profile of the concentration of 30 nm particles at the blast fence while an aircraft prepared for takeoff from LAX. The aircraft traveled east on the 25R taxiway to the blast fence for departure. As shown in Fig. 3, the concentrations of 30 nm particles gradually increased from a baseline level ~40 particles cm^{-3} to ~2800 particles cm^{-3}. Upon arrival near the blast fence, the aircraft made a 180-degree turn from the taxiway (facing east) onto the 25R runway (facing west). The jet blast rotated in a clockwise direction from the west to the east, resulting in a slight decrease in particle concentration. Following the 180-degree turn, the pilot initiated takeoff, increasing the engine thrust level. The concentration of 30 nm particles dramatically elevated from 1560 particles cm^{-3} to 17,200 particles cm^{-3}, a more than 10-fold increase. The aircraft accelerated along the runway, traveling toward the west away from the sampling location, continuously emitting particles that were blown by jet blast and transported by prevailing wind toward the blast fence. The particles in this case were dispersed and their number concentrations exhibited decay characteristics that were described by exponential decay according to the following equation:

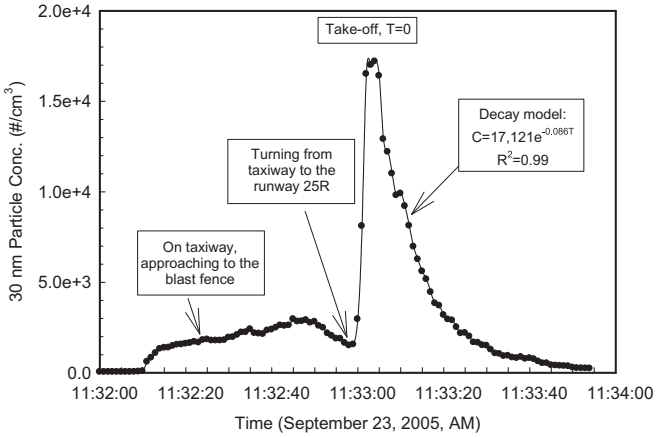

Fig. 3. Temporal profile of 30 nm particles during a takeoff event.

$$C = C_0 \times \exp(-kt) = 17,121 \times \exp(-0.08575 \times t) \quad (2)$$

with $R^2 = 0.9927$, where $t = 0$ is the second when the takeoff was initiated and C_0 (particles cm^{-3}) represents a characteristic constant for emissions of 30 nm particles for a specific takeoff event which depends upon the particle size and individual aircraft. The model constant k indicates particle dispersion characteristics, which depends upon meteorological factors. Although the temporal profile in taxiing and idling prior to takeoff may vary substantially with specific events, the overall pattern of decay associated with takeoffs was very similar for different particle sizes and aircrafts. We have randomly selected 112 peaks for different particle sizes between 10 and 50 nm and fit an exponential decay curve for each peak. The amplitudes of the decay curves (C_0) varied greatly with respect to aircraft and particle size, but the exponents of different peaks (k) were fairly constant with a mean value of −0.049 (SD = 0.018). The R^2 values were all greater than 0.94 for the peaks we analyzed, indicating a rapid exponential decay is a good fit for particle number concentrations during takeoffs.

For each of the particle sizes monitored at the blast fence, the temporal profile of measured concentration was highly variable. These peaks were associated with aircraft takeoffs, confirmed by inspection of LAX aircraft activity logs. Fig. 4 presents temporal profiles of 15 nm particles as measured simultaneously at the blast fence and 170 m downwind from the blast fence, which was 310 m from the source (the point on runway 25R at which takeoff is typically initiated). In Fig. 4, time series of 15 nm particle number concentrations were plotted and compared with the log file of aircraft activities. Each identified peak was plotted individually on a broader time scale as in Fig. 3. The peak which occurred closest to an aircraft takeoff event was assigned to this aircraft activity. In general, there were dramatic increase and decrease in the observed peaks when an aircraft took off, for example # 1 in Fig. 4. Occasionally, more than one peak occurred immediately next to each other, for example # 6 in Fig. 4. Since there was no aircraft activity within such a short time frame, these sub-peaks were attributed to a single aircraft takeoff event. The start point of a peak was defined as the lowest value when the sharp increase began and the end point was the lowest value after the sharp decrease ended. The time between these two points was defined as the interval of a peak.

Data shown in Fig. 4(a) and (b) were collected simultaneously during a period of approximately 30 min. The time profiles are very similar. The spikes of particles are those associated with takeoff events, noted in the figure by numerals. Table 2 lists the aircraft activity noted by LAX during this period, for comparison with the figure. Takeoff spikes of UFP were clearly detected at the downwind site, with a time lag of approximately 20 s. Note that during the time period when there were no takeoffs, there were no spikes at either the blast fence or downwind location.

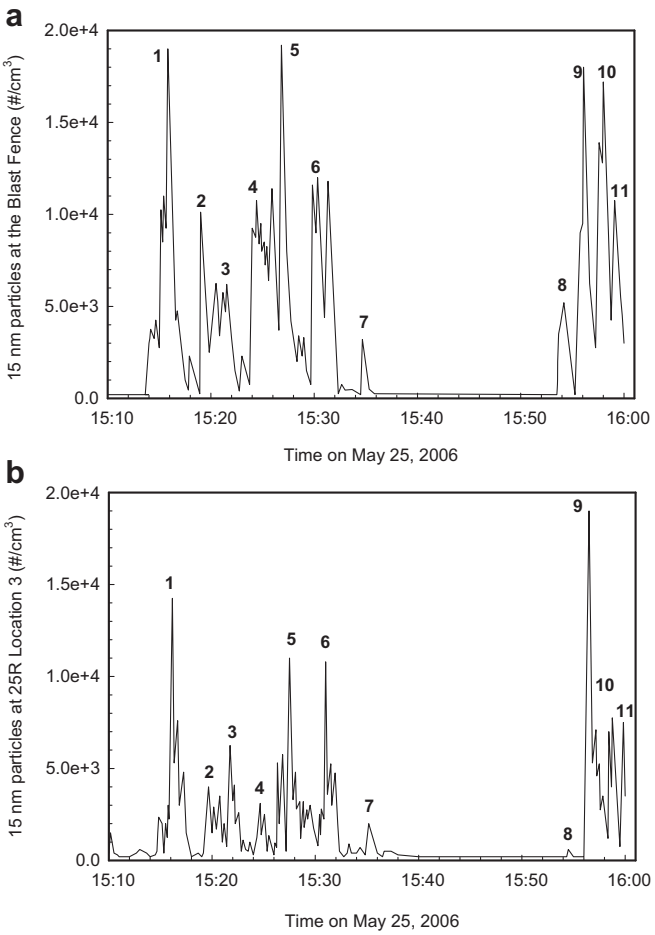

Fig. 4. Temporal profile of 15 nm particle concentrations at (a) the LAX blast fence and (b) a 170 m downwind site of the blast fence during the same time period. Aircraft departures logged by LAX are noted with numerals, see Table 2 for details.

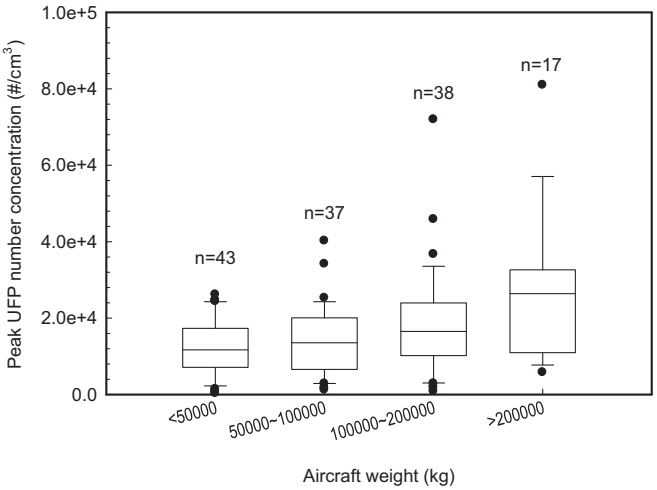

Fig. 5. Peak concentrations of 15 nm particles observed during takeoff events with respect to different aircraft weights.

Fig. 4 shows the variation in particle concentrations emitted from various aircraft taking off during the monitored time period. In the absence of a takeoff event, 15 nm particle concentrations ranged from 60 to 150 particles cm^{-3}, the baseline of the time profile in Fig. 4. During takeoff, aircraft generated large numbers of particles, ranging up to 28,000 particles cm^{-3}, a 100-fold increase from background levels.

Particle concentration data of other studied sizes showed a similar temporal pattern of peaks associated with aircraft activity to that in Fig. 4. In addition, the peak-tracking pattern observed between the blast fence site and the 170 m downwind site holds to 600 m downwind which is the furthest sampling site used in the study. Downwind peaks were usually observed within seconds after aircraft takeoffs indicating that aircraft exhaust plumes can travel considerable distances. Because the exhaust plume from aircraft takeoff was emitted forcefully in the direction of the prevailing wind, it took less time for the plume to reach the air samplers, and the air dilution is therefore minimal. This is in contrast to the crosswind passive dispersion of vehicular exhaust from freeway traffic in which UFPs were decayed within a few hundred meters downwind of the freeway (Zhu et al., 2002a, b).

3.3. Ultrafine particle emissions during takeoff activities

The number concentrations of 15 nm particle from February 23 to March 2, 2006 were used to analyze the contribution of aircraft weight to UFP emissions at the LAX runway. Maximum takeoff weight (MTOW) derived from aircraft performance database (Aircraft performance database V2.0, 2011) was used as the aircraft weight. It should be noted, that it was likely not all aircrafts were at MTOW or used full thrust during the phase of activity on the runway. Given the limited information regarding aircraft performance and hence engine power settings, we choose to arbitrarily classify the aircrafts studied during this study into four weight categories: less than 50,000 kg, 50,000–100,000 kg, 100,000–200,000 kg, and greater than 200,000 kg. In addition, fuel composition may also affect particle emission characteristics. Because aircrafts at LAX all use local fuel, we assumed that the fuel being burned by each aircraft was the same. From time series plots every peak associated with aircraft takeoff events at 25R runway was identified. The selected concentration peaks have typical shapes, as shown in Fig. 3, which increase rapidly and decay to background level with a short tail of 30–90 s. The peaks with longer tails may be generated by other airport activities and not included in the analysis. The mean peak height of 15 nm particle in relation to different aircraft weight was shown in Fig. 5. Numbers of observed peaks (n) were also indicated in Fig. 5.

The mean peak height of 15 nm particle increased slightly with aircraft weight. Light aircrafts with MTOW less than 50,000 kg emitted the lowest amount of 15 nm particles, of which the mean peak height was 11,900 particles cm^{-3}. The aircrafts with MTOW of 50,000–100,000 kg and 100,000–200,000 kg

Table 2
Aircraft departures on runway 25R associated with data profiled in Fig. 4.

Label	1	2	3	4	5	6	7	8	9	10	11
Time	15:15	15:17	15:19	15:22	15:23	15:26	15:31	15:50	15:52	15:54	15:55
Aircraft Type	B744	B752	F2TH	A320	B744	B737	MD83	SF34	B744	B738	B763
MTOW ($\times 10^3$ kg)[a]	397	113	16	78	397	52	64	13	397	79	187

[a] MTOW: Maximum takeoff weight.

emitted 1800 particles cm^{-3} and 4800 particles cm^{-3} more, respectively. Heaviest aircrafts emitted the largest amount, with an average peak concentration of 26,500 particles cm^{-3}. Similar UFP emission trend with respect to aircraft weight has been reported for Santa Monica Airport (SMA) in which greater fuel consumption rates were associated with heavy aircrafts during takeoff (Hu et al., 2009). It should also be noted, there were only 135 peaks analyzed in Fig. 5 which may cause some uncertainty in the results. A further study and analysis with more data is necessary to make an improved conclusion on the effect of aircraft weight on UFP emissions.

By integrating the total number concentration of UFP peaks in relation to takeoff events, the relative contributions of aircraft activities were analyzed. From February 28, 2006 to March 3, 2006, aircraft takeoffs contributed 53.5% to the total UFP concentration at the blast fence of 25R runway, other airport operations contributed 45.8% and the background ambient accounted for 0.7%. Other airport operations include landing, taxi, idle and ground vehicles operation, while the data of background level were from the measurements at the upwind AQMD background site. During takeoff, high engine thrust and large fuel consumption are required to produce enough power for aircraft lift-up which generate greater amount of UFPs than the other activities.

The SMPS data and CO_2 concentrations concurrently collected on September 23, 2005 at the blast fence were used to calculate emission index, EI_{pm}, of takeoff activities. Fig. 6 shows typical time series of particle and CO_2 levels at the blast fence. It is clear, for each takeoff, both CO_2 and particle concentrations increased sharply and then decayed quickly. For a given size (30 nm particles in Fig. 6), every particle and CO_2 concentration peak with typical curve (sharp increase and fast decay, Fig. 3.) associated with individual aircraft takeoff event was identified from the time series measurements. The average particle number and CO_2 concentration was obtained by dividing the sum of particle and CO_2 concentration reading by the time interval of the peak. After subtracting the background levels, the average concentrations were assigned as the particle and CO_2 index to this peak. Eq. (1) was then used to calculate EI_{pm} for each takeoff for the studied particle size, 30 nm particles in this case. The mean value and the standard deviation from multiple takeoff events were obtained. This process was then repeated for each studied particle size and the results were shown in Fig. 7.

Fig. 7 presents a clear match between EI_{pm} and the size distribution at the blast fence. The size distribution has the major peak number concentration occurring at 15 nm. For particles smaller than 20 nm, EI_{pm} increases with diameters, and then decreases

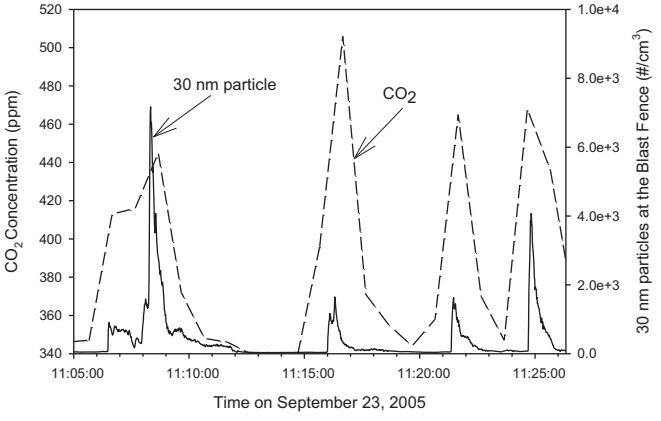

Fig. 6. Typical temporal profiles of CO_2 and 30 nm particle concentrations at the LAX blast fence on Sep 23, 2005.

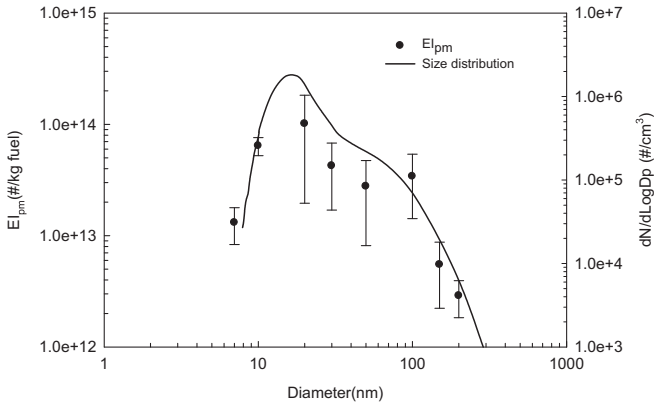

Fig. 7. Calculated EI_{pm} (left *Y*-axis) for takeoff activities on Sep 23, 2005 at the LAX runway, compared with particle size distribution (right *Y*-axis) at the blast fence. Size distribution was aggregated from SMPS scans on Sep 23, 2005.

when the size grows. Therefore EI_{pm} could be used as a predictor of particles emitted by aircraft takeoff events, combined with fuel consumption. EI_{pm} for specific diameters were integrated to get EI_{pm} of the total number concentration in the size range of 7 nm–320 nm which is approximately 3.4×10^{16} particles/(kg fuel). This value is larger than the average *EI*s measured a JFK airport (1.0×10^{14} particles/(kg fuel)) (Herndon et al., 2005). At JFK, the average *EI*s were calculated based on particle size distribution data collected with an Electrical Low Pressure Impactor in the size range of 30–10,000 nm. Since a large proportion of UFPs from aircraft takeoff emissions were found smaller than 30 nm in this study, it is not surprising to obtain a much higher EI at LAX than JFK. The EIs observed in this study are also comparable with data reported at Logan airport (8.8×10^{15} particles/(kg fuel)) (Herndon et al., 2005) and SMA in Southern California (5.0×10^{16} particles/(kg fuel)) (Hu et al., 2009) where similar instruments were used that detect particles smaller than 30 nm.

3.4. Spatial decay profiles of 15 nm particles and black carbon

Fig. 8 presents the distributions of number concentrations of 15 nm particles and BC concentrations measured at increasing distances downwind of the departure runway, 25R. The box plots summarize all data (Fig. 8a and c) and the top quartile of data (Fig. 8b and d) collected during prevailing wind conditions at the blast fence and downwind locations 1 through 5 (see Fig. 1 for locations). Plotting the top quartile of concentrations is a surrogate for manually inspecting the time series profiles of the data and selecting those concentration peaks that are associated with aircraft departures. The observed UFP and BC concentrations are highly variable due to the emission variability from individual aircraft. Average number concentrations of 15 nm particles and mass concentrations of BC decrease remarkably with increasing distance from the runway mainly because of the atmospheric dispersion process. Nevertheless, concentrations of BC and 15 nm particles observed at 600 m downwind from the runway remain elevated compared to the AQMD background site. The observed decay was greater and stronger for upper quartile data as indicated by fitted slope and R^2 values. Previously we have shown UFP and BC concentrations return to background by about 300 m downwind of major Southern California freeways during daytime (Zhu et al., 2002a, b). Data collected from the current study suggest airport emissions have a much broader spatial impact on local air quality comparing to urban freeways. Similar to our observation, elevated UFP concentrations, 2.5–3 times the background, were reported

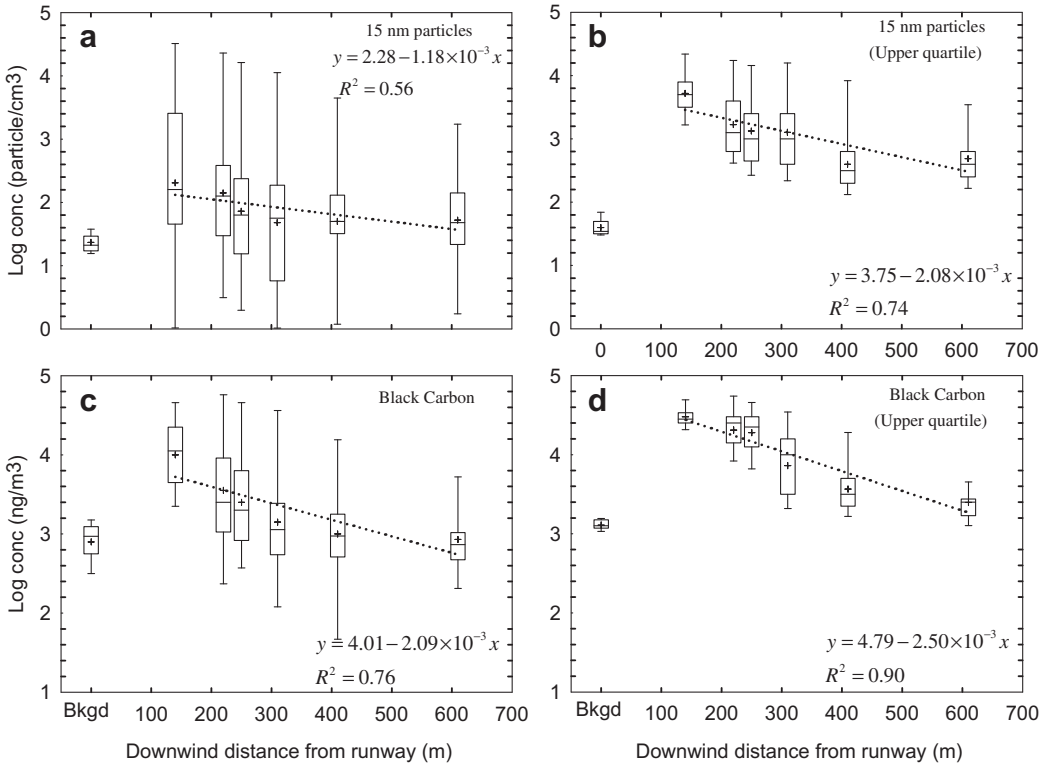

Fig. 8. Concentrations of (a) 15 nm particles, (b) upper quartile of 15 nm particles, (c) black carbon and (d) upper quartile of black carbon downwind of runway 25R. Locations are described in meters from aircraft takeoff positions. The first sampling location, blast fence, is at 140 m. The background (Bkgd) levels were the averaged concentrations measured at the blast fence when there was no aircraft activity.

near a general aviation airport in Southern California (Hu et al., 2009). These observations confirm the broader spatial impacts of high numbers of UFPs emitted from aircraft during takeoff.

3.5. $PM_{2.5}$, polycyclic aromatic hydrocarbons, and volatile organic compounds

Time averaged mass concentrations of $PM_{2.5}$, particle- and vapor-phase PAHs, and four VOCs are shown in Table 3. The mean concentration at the LAX blast fence during the September study was $37.1 \pm 15.4\ \mu g\ m^{-3}$, significantly greater ($p < 0.001$) than concentrations measured at the background site ($14.3 \pm 10.4\ \mu g\ m^{-3}$). Daily mean $PM_{2.5}$ concentrations of the LAX site varied between 32 and 42 $\mu g\ m^{-3}$ and were consistently significantly greater than the daily means $PM_{2.5}$ concentrations at the AQMD site (9–18 $\mu g\ m^{-3}$)($P < 0.001$ for daily comparisons).

Naphthalene comprised 80–85% of the total vapor-phase PAH mass at both sites. Higher naphthalene levels were found at the LAX blast fence than at the AQMD site. Overall, the levels of vapor-phase PAH were consistently higher at the LAX blast fence than at background site. Particle-phase PAH also differed between the two sites. The semi-volatile PAHs (from phenanthrene to chrysene) were consistently higher at the LAX blast fence than the background site. On the other hand, the high molecular weight PAHs (from benzo[*a*]pyrene to indeno[*1,2,3-cd*]pyrene) were lower at the blast fence than the background site. The differences in concentrations of individual particle- and vapor-phase PAHs between the two sites are not statistically significant, but there is a clear trend in the differences of PAHs at blast site compared to control for the lower molecular weight PAHs. It is also noted, a greater amount of PAHs were in the vapor phase than in the particle phase. This is especially true for naphthalene which indicates its potential for greater health effects.

Table 3
$PM_{2.5}$ mass, particle- and vapor-phase PAH, and VOC concentrations at AQMD background site and the LAX blast fence.

Phase	Species	AQMD		LAX_BF	
		Mean	SD	Mean	SD
Unit: $\mu g\ m^{-3}$					
Particle	$PM_{2.5}$	14.3	10.4	37.1	15.4
Unit: $pg\ m^{-3}$	PAHs				
Particle	Naphthalene	–	–	14.1	–
	Fluorene	13.7	–	–	–
	Phenanthrene	111.1	88.1	175.6	54.6
	Anthracene	4.7	3.4	10.5	7.4
	Fluoranthene	91.0	117.3	161.7	48.8
	Pyrene	106.1	113.4	134.7	63.1
	Benz[a]anthracene	23.0	19.7	36.4	34.7
	Chrysene	48.4	46.1	78.2	55.7
	Benzo[b]fluoranthene	55.6	38.3	56.0	42.8
	Benzo[k]fluoranthene	22.9	17.9	18.7	15.5
	Benzo[a]pyrene	46.7	43.0	28.1	33.2
	Dibenz[a,h]anthracene	7.5	6.1	2.7	0.6
	Benzo[ghi]perylene	121.2	101.0	49.0	57.1
	Indeno[1,2,3-cd]pyrene	48.5	36.0	18.3	15.7
Unit: $ng\ m^{-3}$					
Vapor	Naphthalene	55.8	55.9	82.5	64.5
	Acenaphthene	1.4	1.9	2.8	1.7
	Fluorene	2.1	2.4	4.7	1.9
	Phenanthrene	2.0	1.7	4.8	1.8
	Anthracene	0.1	0.1	0.4	0.2
	Fluoranthene	0.4	0.1	0.8	0.2
	Pyrene	0.5	0.2	1.1	0.5
	Benz[a]anthracene	0.2	0.1	0.2	0.1
Unit: ppb	VOCs				
Vapor	Acrolein	1.03	0.35	1.26	0.08
	Benzene	0.42	0.29	0.52	0.57
	1,3-Butadiene	0.15	0.08	0.36	0.23
	Formaldehyde	0.53	0.22	1.70	0.66

The mean concentration of formaldehyde at the blast fence was significantly (3-fold) higher than that at the AQMD background site ($p = 0.006$). This is likely because formaldehyde constitutes a large fraction of total aircraft gaseous emissions (Kinsey, 2009). Acrolein was also higher at LAX blast fence than at the background site ($p = 0.034$). There were no statistically significant differences in concentrations of benzene or butadiene between the two monitoring sites, but there were increased average concentrations for these organic compounds over the control site and most of the other VOCs were below the limit of detection (LOD) even at the blast fence site. Furthermore, for those VOCs above detection limit, no significant differences were seen between the two sites other than those presented in Table 3.

4. Conclusions

Data collected immediately downwind of aircraft takeoff at LAX showed very high number concentrations of UFP, with the highest numbers found at a particle size of approximately 14 nm. The highest spikes in the time profile of UFP number concentrations were clearly correlated with aircraft takeoff events. Total UFP counts exceeded 10^7 cm^{-3} during some monitored takeoffs. Time averaged concentrations of $PM_{2.5}$ mass and two carbonyl compounds, formaldehyde and acrolein, were elevated at LAX relative to a background reference site. The results of the project demonstrate that in-use commercial aircraft at LAX emit large quantities of UFPs at the lower end of currently measurable particle size ranges. Spikes of 15 nm particles can be detected and associated temporally with aircraft activity up to 600 m east of the airport.

Acknowledgment

We thank the Los Angeles World Airports (LAWA) who granted access to the airfield runway location. We thank Dr. Arantza Eiguren-Fernandez for analysis of the PAH data and helpful discussion. We also thank the South Coast Air Quality Management District who provided access to their monitoring site near Hastings/Westchester Blvd, Los Angeles. This study was supported by California Air Resource Board (Contract # 04-325) and the Southern California Particle Center (EPA grant #RD-83241301).

References

Aircraft performance database V2.0, 2011. http://elearning.ians.lu/aircraftperformance/.

Boldo, E., Medina, S., LeTertre, A., Hurley, F., Mucke, H.G., Ballester, F., Aguilera, I., Eilstein, D., 2006. Apheis: health impact assessment of long-term exposure to PM2.5 in 23 European cities. European Journal of Epidemiology 21, 449–458.

Diapouli, E., Chaloulakou, A., Spyrellis, N., 2007. Levels of ultrafine particles in different microenvironments – implications to children exposure. Science of the Total Environment 388, 128–136.

Eiguren-Fernandez, A., Miguel, A.H., Froines, J.R., Thurairatnam, S., Avol, E.L., 2004. Seasonal and spatial variation of polycyclic aromatic hydrocarbons in vapor-phase and PM 2.5 in Southern California urban and rural communities. Aerosol Science and Technology 38, 447–455.

Garnier, F., Baudoin, C., Woods, P., Louisnard, N., 1997. Engine emission alteration in the near field of an aircraft. Atmospheric Environment 31, 1767–1781.

Hasegawa, S., Wakamatsu, S., Ohara, T., Itano, Y., Saitoh, K., Hayasaki, M., Kobayashi, S., 2007. Vertical profiles of ultrafine to supermicron particles measured by aircraft over Osaka metropolitan area in Japan. Atmospheric Environment 41, 717–729.

Herndon, S.C., Onasch, T.B., Frank, B.P., Marr, L.C., Jayne, J.T., Canagaratna, M.R., Grygas, J., Lanni, T., Anderson, B.E., Worsnop, D., Miake-Lye, R.C., 2005. Particulate emissions from in-use commercial aircraft. Aerosol Science and Technology 39, 799–809.

Hu, S., Fruin, S., Kozawa, K., Mara, S., Winer, A.M., Paulson, S.E., 2009. Aircraft emission impacts in a Neighborhood adjacent to a general aviation airport in Southern California. Environmental Science & Technology 43, 8039–8045.

Kinsey, J.S., 2009. Characterization of Emissions from Commercial Aircraft Engines during the Aircraft Particle Emissions eXperiment (APEX) 1 to 3. U.S. Environmental Protection Agency, Research Triangle Park, NC, p. 227.

Kinsey, J.S., Dong, Y.J., Williams, D.C., Logan, R., 2010. Physical characterization of the fine particle emissions from commercial aircraft engines during the Aircraft Particle Emissions eXperiment (APEX) 1-3. Atmospheric Environment 44, 2147–2156.

Li, N., Hao, M.Q., Phalen, R.F., Hinds, W.C., Nel, A.E., 2003a. Particulate air pollutants and asthma – a paradigm for the role of oxidative stress in PM-induced adverse health effects. Clinical Immunology 109, 250–265.

Li, N., Sioutas, C., Cho, A., Schmitz, D., Misra, C., Sempf, J., Wang, M.Y., Oberley, T., Froines, J., Nel, A., 2003b. Ultrafine particulate pollutants induce oxidative stress and mitochondrial damage. Environmental Health Perspectives 111, 455–460.

Oberdorster, G., Sharp, Z., Atudorei, V., Elder, A., Gelein, R., Kreyling, W., Cox, C., 2004. Translocation of inhaled ultrafine particles to the brain. Inhalation Toxicology 16, 437–445.

Pope, C.A., Dockery, D.W., 2006. Health effects of fine particulate air pollution: lines that connect. Journal of the Air & Waste Management Association 56, 709–742.

Possanzini, M., Di Palo, V., Tagliacozzo, G., Cecinato, A., 2006. Physico-chemical artefacts in atmospheric PAH denuder sampling. Polycyclic Aromatic Compounds 26, 185–195.

Schwarze, P.E., Ovrevik, J., Lag, M., Refsnes, M., Nafstad, P., Hetland, R.B., Dybing, E., 2006. Particulate matter properties and health effects: consistency of epidemiological and toxicological studies. Human & Experimental Toxicology 25, 559–579.

Westerdahl, D., Fruin, S., Sax, T., Fine, P.M., Sioutas, C., 2005. Mobile platform measurements of ultrafine particles and associated pollutant concentrations on freeways and residential streets in Los Angeles. Atmospheric Environment 39, 3597–3610.

Westerdahl, D., Fruin, S.A., Fine, P.L., Sioutas, C., 2008. The Los Angeles International Airport as a source of ultrafine particles and other pollutants to nearby communities. Atmospheric Environment 42, 3143–3155.

Yu, K.N., Cheung, Y.P., Cheung, T., Henry, R.C., 2004. Identifying the impact of large urban airports on local air quality by nonparametric regression. Atmospheric Environment 38, 4501–4507.

Zhu, Y.F., Hinds, W.C., Kim, S., Shen, S., Sioutas, C., 2002a. Study of ultrafine particles near a major highway with heavy-duty diesel traffic. Atmospheric Environment 36, 4323–4335.

Zhu, Y.F., Hinds, W.C., Kim, S., Sioutas, C., 2002b. Concentration and size distribution of ultrafine particles near a major highway. Journal of the Air & Waste Management Association 52, 1032–1042.